

Extremal climatic states simulated by a 2-dimensional model

Part I: Sensitivity of the model and present state

By TONI PUJOL*^{1,2} and JOSEP ENRIC LLEBOT², ¹*Dept. de Física, Facultat de Ciències, Universitat de Girona, 17071 Girona, Catalonia, Spain;* ²*Dept. de Física, Facultat de Ciències, Universitat Autònoma de Barcelona, 08193 Bellaterra, Catalonia, Spain*

(Manuscript received 7 May 1999; in final form 28 January 2000)

ABSTRACT

The criterion, based on the thermodynamics theory, that the climatic system tends to extremize some function has suggested several studies. In particular, special attention has been devoted to the possibility that the climate reaches an extremal rate of planetary entropy production. Due to both radiative and material effects contribute to total planetary entropy production, climatic simulations obtained at the extremal rates of total, radiative or material entropy production appear to be of interest in order to elucidate which of the three extremal assumptions behaves more similar to current data. In the present paper, these results have been obtained by applying a 2-dimensional (2-Dim) horizontal energy balance box-model, with a few independent variables (surface temperature, cloud-cover and material heat fluxes). In addition, climatic simulations for current conditions by assuming a fixed cloud-cover have been obtained. Finally, sensitivity analyses for both variable and fixed cloud models have been carried out.

1. Introduction

From a thermodynamic viewpoint, the parameters in the final equilibrium of a system with many degrees of freedom may be expected to extremize some function. Therefore, several extremal hypotheses have been applied to a global picture of the climatic system, where in comparison with thermodynamics theory, an expression related to the entropy would seem to be a suitable constraint. However, the climatic entropy is formed by two contributions with different properties (material and radiation), fact that complicates these types of analyses. Examples of climatic states obtained at maximum rates of material entropy production can be found in Paltridge (1975),

Grassl (1981), and O'Brien and Stephens (1995) in a 1-Dim horizontal box-model, and in Wyant et al. (1988), and Pujol and Llebot (1999a) in 1-Dim horizontal diffusive models. The hypothesis that the climate leads to a minimum state of radiative entropy production, which can be related to one of Planck's results (Planck, 1913), has been used by Essex (1984), and Pujol and Llebot (1999b), who have also analyzed the climate at the extremal rate of total entropy production (i.e., material plus radiative parts). Moreover, based on the suggestion that the convective heat transfer tends to the maximum efficiency, Paltridge (1978) introduces the hypothesis of maximum convection, with reference to the behaviour of latent- plus sensible-heat fluxes.

Although some authors (Paltridge, 1979) have tried to justify the application of the above hypotheses to the climatic system, none of them

* Corresponding author.
e-mail: caaps@fc.udg.es

has been fully demonstrated. Furthermore, some questions arise from previous results: (1) it seems that the application of extremal principles to the climate could depend on the structure of the model. For example, latitudinal temperature distribution substantially varies when applying the same extremal principle to different climatic models (compare, e.g., Pujol and Llebot, 1999a–b); (2) O'Brien and Stephens (1995) point out the possible relevance of the convective hypothesis in those studies that include both maximum convection and dissipation principles (Paltridge, 1978, 1981; O'Brien and Stephens, 1995; Pujol and Llebot, 1999b). Thus, it is important to quantify the influence of the maximum convection hypothesis in defining the climate reached by the system; (3) the fundamental question, however, remains the same as in Paltridge's earliest analysis (Paltridge, 1975): is the real climatic system governed by any of the above extremal principles?

With the aim of giving answers to these questions, a 2-Dim horizontal box-model based on Paltridge's energy balance model (EBM; Paltridge, 1978) has been used. This model has been described in Section 2. The results for present conditions at maximum dissipation (i.e., at maximum rate of entropy production) have been obtained with and without using the hypothesis of maximum convection (i.e., by considering variable or fixed cloud-cover respectively), whereupon the relevance of the convective hypothesis has been analyzed (Section 3). Moreover, the results have been compared with those obtained by using a 1-Dim version of the box-model as well as with those deduced from 1-Dim diffusive EBMs. Thus, the dependence of the extremal hypotheses on both dimension and structure of the model has been observed.

The effect of the ice-albedo feedback for both maximum dissipation and convection is shown in Section 4, where the sensitivity analysis has been included. Finally, we resume the main conclusions in Section 5. Although no general justification has been found for the application of extremal hypotheses, several climatic simulations for different scenarios have been obtained in Part II. Then, the similarities with observed data or projected states simulated by more complex models can provide additional support for the extremal principles proposed.

2. Model

2.1. Description

The 2-Dim horizontal model is formed by 1024 boxes that cover the entire globe, with 32 latitudinal and 32 longitudinal divisions. Each box has an equal surface area and occupies 11.25° of longitude, the meridional division being variable. Moreover, each cell has been subdivided into oceanic and atmospheric regions. Four free-variables must be found in each box: surface temperature T , cloud-cover ϑ , convective heat fluxes $LE + H$ and advective heat fluxes X (oceanic X_o , plus atmospheric X_a). Cloud-cover represents an average value of cloud types and their properties, and all the parameters and variables refer to annual mean values. We must stress the very schematic picture of the climatic system provided by this model, without taking into account several mechanisms that are fundamental in the description of the climate (e.g., wind field). Thus the climate dynamics has been represented by the distribution of both advective and convective heat fluxes, which have been obtained by using the extremal hypotheses. Short- and long-wave energy radiation fluxes are defined at the top of the atmosphere (TOA) and at the surface. Short-wave energy radiation at TOA H_{ST} , takes the albedo of cloudy ω_{ct} and clear-sky ω_{gt} regions at TOA into account,

$$H_{ST} = -\varepsilon[(1 - \omega_{gt})(1 - \vartheta) + (1 - \omega_{ct})\vartheta]F, \quad (1)$$

where ω_{gt} and ω_{ct} consider the reflection of incoming radiation from the surface,

$$\omega_{gt} = \omega_g + \alpha_s(1 - \omega_g)(1 - \underline{\omega}_g)(1 - \alpha_a)(1 - \underline{\alpha}_a), \quad (2a)$$

$$\omega_{ct} = \omega_c + \alpha_s(1 - \omega_c)(1 - \underline{\omega}_c)(1 - \alpha_a)(1 - \underline{\alpha}_a), \quad (2b)$$

α_s being the surface albedo, ω_g the clear-sky albedo and ω_c the cloudy albedo. The underbar in (2a–b) refers to diffusive components, whereas α_a represents the absorption by gases in the atmosphere and $\underline{\omega}_c$ takes the effect of the absorption due to water droplets α_c into account. In eq. (1), F is the solar "constant" $\approx 1360 \text{ W m}^{-2}$ and ε the annual average of the cosine of the solar zenith angle at latitude φ (O'Brien and Stephens, 1995).

Short-wave energy radiation at the surface H_{SS} is defined as

$$H_{SS} = -\varepsilon[(1 - \omega_{gs})(1 - \vartheta) + (1 - \omega_{cs})\vartheta]F, \quad (3)$$

where ω_{gs} and ω_{cs} are the clear-sky and the cloudy albedo at the surface respectively. Both values follow Paltridge (1978), being

$$\omega_{gs} = \omega_g + \alpha_s + \alpha_a, \quad (4a)$$

$$\omega_{cs} = \omega_c + \alpha_s + \alpha_a + \alpha_c. \quad (4b)$$

Long-wave radiation is expressed in terms of surface temperature. Thus, the long-wave energy radiation H_{LT} at TOA is

$$H_{LT} = (m_g + m_a)(1 - \vartheta)\sigma_{St}T^4 + m_c\vartheta\sigma_{St}T^4, \quad (5)$$

where for the clear-sky region, m_a and m_g correspond to the atmospheric emissivity and to the fraction of surface radiation which is directly lost to space respectively. For the cloudy region, m_c is related to the cloud-top emissivity. In eq. (5), σ_{St} is the Stefan constant.

Long-wave energy radiation at the surface H_{LS} can be written as

$$H_{LS} = m_g(1 - \vartheta)\sigma_{St}T^4 + (m_g - n_c)\vartheta\sigma_{St}T^4, \quad (6)$$

where n_c is related to the emissivity of cloud-base downward radiation.

From (1) and (5), the energy balance equation for one cell (atmosphere plus ocean) is

$$\begin{aligned} & (m_g + m_a)(1 - \vartheta)\sigma_{St}T^4 + m_c\vartheta\sigma_{St}T^4 \\ & - \varepsilon[(1 - \omega_{gt})(1 - \vartheta) + (1 - \omega_{ct})\vartheta]F + \Delta X = 0, \end{aligned} \quad (7)$$

where material heat fluxes only correspond to advection (X) since convection ($LE + H$) is a flux located inside the cell (from ocean-surface to atmosphere).

From (3) and (6), the energy balance equation for the ocean yields

$$\begin{aligned} & m_g(1 - \vartheta)\sigma_{St}T^4 + (m_g - n_c)\vartheta\sigma_{St}T^4 \\ & - \varepsilon[(1 - \omega_{gs})(1 - \vartheta) + (1 - \omega_{cs})\vartheta]F \\ & + \Delta X_o - (LE + H) = 0, \end{aligned} \quad (8)$$

where ΔX_o refers to oceanic advective heat fluxes (meridional and longitudinal). The energy balance equation for the atmosphere can be obtained from (7) minus (8).

Following O'Brien and Stephens (1995), eqs. (7) and (8) can be expressed as

$$A - B\vartheta - \eta(C - D\vartheta) + \zeta = 0, \quad (9)$$

$$P - Q\vartheta - \eta(R - S\vartheta) + \zeta_o - q = 0, \quad (10)$$

where the parameters A , B , P and Q for the short-wave radiation and C , D , R and S for the long-wave radiation are

$$A = \varepsilon(1 - \omega_{gt}), \quad B = \varepsilon(\omega_{ct} - \omega_{gt}), \quad (11a-b)$$

$$P = \varepsilon(1 - \omega_{gs}), \quad Q = \varepsilon(\omega_{cs} - \omega_{gs}), \quad (11c-d)$$

$$C = m_g + m_a, \quad D = m_g + m_a - m_c, \quad (12a-b)$$

$$R = m_g, \quad S = n_c, \quad (12c-d)$$

and the dimensionless variables η , q and ζ follow

$$\eta = \frac{\sigma_{St}T^4}{F}, \quad \zeta = \frac{\Delta X}{F}, \quad q = \frac{LE + H}{F}, \quad (13a-c)$$

where $\zeta = \zeta_a + \zeta_o$ and $\zeta_i = \Delta X_i/F$, with $i = a, o$.

2.2. Values of the parameters

The parameters are chosen similar to those used by Paltridge (1978) for comparison purposes with previous results based on 1-Dim box-models. Thus, the parameters that do not vary either in latitude or in longitude are shown in Table 1. Cloudy and clear-sky albedos are only a function of latitude and correspond to interpolated and extrapolated values used by Paltridge (1978) (Fig. 1). Finally, the surface albedo α_s is the only parameter that depends on both horizontal directions. The values used for α_s are shown in Fig. 2. Surface albedos at high latitudes have been chosen as an intermediate value of those corresponding to old, melting snow and dry, cold snow (see Hartmann, 1994). The zonally-averaged surface albedo at the polar boxes (from 69.6° to 90° of

Table 1. Values for the parameters that do not vary either in longitude or in latitude (Paltridge, 1978)

	Long-wave		Short-wave
m_a	0.31	α_a	0.14
m_g	0.3	α_c	0.08
m_c	0.6	α_a	0.028
n_c	0.24	ω_c	0.35
		ω_g	0.1

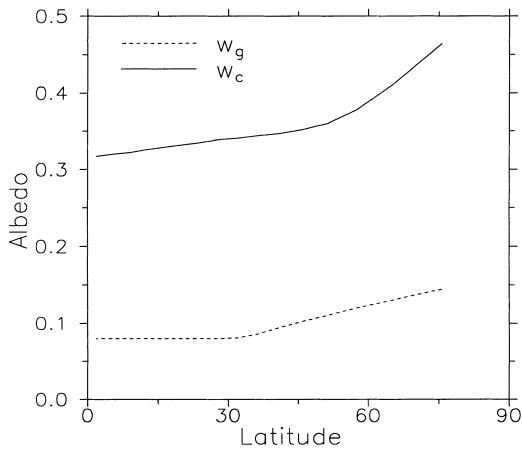


Fig. 1. Latitudinal distribution for clear-sky albedo w_g and cloudy albedo w_c .

latitude) gives a value of $\alpha_s \approx 0.63$ at the Southern Hemisphere and 0.59 at the Northern Hemisphere, following the values of the ice-albedo found in simple EBMs (Nicolis and Nicolis, 1981).

2.3. Ice-albedo feedback

Grassl (1981) includes the ice-albedo feedback in a 1-Dim box-model similar to that used here. However, this author does not take the convective hypothesis into account (i.e., the maximum convection requirement). Here, the ice-albedo feedback is introduced in a simple way, by accepting a dependence of surface albedo on temperature

through the parameter b defined as

$$b = \frac{\partial \alpha_s}{\partial T} = \frac{d\alpha_s}{dT} - \frac{\partial \alpha_s}{\partial \mu} \frac{d\mu}{dT}, \tag{14}$$

where μ represents the cosine of the solar zenith angle.

The coefficient $d\mu/dT$ can be easily deduced (North, 1975), whereas $d\alpha_s/dT$ and $\partial \alpha_s / \partial \mu$ have been obtained from Lian and Cess (1977). Hence, b is not a constant value as used by Källén et al. (1979), or Ghil and Le Treut (1981), but a function of latitude, which has been applied for latitudes φ beyond 55° and surface temperatures T lower than 273.15 K (Roesch et al., 1999). However, the results at high latitudes do not vary substantially when taking a constant value of b . Thus, sensitivity studies and analyses for different scenarios produce similar results for constant values of b ranging between $-2 \times 10^{-3} \text{ K}^{-1}$ and $-5 \times 10^{-3} \text{ K}^{-1}$.

2.4. Extremization procedure

Energy balance equations (9) and (10) provide two independent expressions for each cell. The other two equations for resolving the four free-variables are obtained by applying two extremal hypotheses. O'Brien and Stephens (1995) show that the hypothesis of maximum convection can be analyzed separately from the hypothesis of maximum dissipation (i.e., maximum rate of entropy production). Thus temperature and cloud-cover which maximize q from (10) and (9)

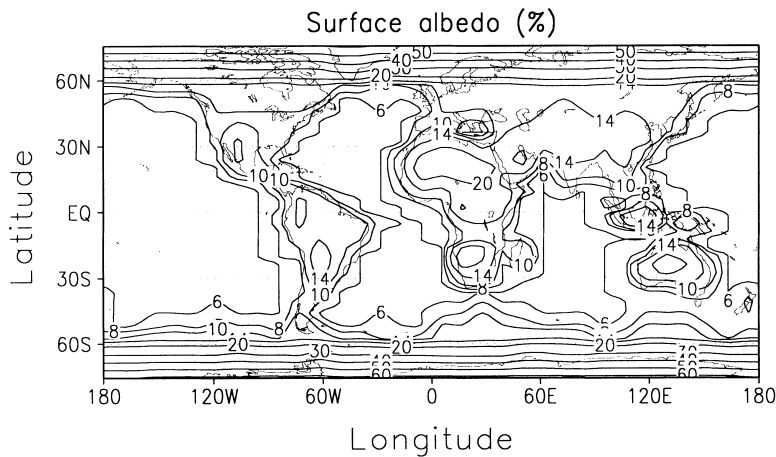


Fig. 2. Distribution of surface albedo α_s in percent.

satisfy

$$\eta = \frac{B - H\sqrt{\gamma}}{D}, \quad (15)$$

$$g = \frac{C - H^{-1}\sqrt{\gamma}}{D}, \quad (16)$$

where H and γ are defined as

$$H = \sqrt{\frac{BS - DQ}{CS - DR}}, \quad (17)$$

$$\gamma = BC - AD - \zeta D. \quad (18)$$

On the other hand, several extremal principles related to the rate of entropy production can be applied. For example, Paltridge (1975) hypothesizes that the climate reaches the maximum rate of material entropy production (Paltridge, 1975), based on Prigogine's principle applied in many thermodynamic systems (Prigogine, 1947). Although the underlying constraints that fulfil this principle are not observed in the climatic system, several authors have analyzed the climatic states at the maximum rates of material entropy production, and among them; Paltridge (1975; 1978; 1981), Grassl (1981), and O'Brien and Stephens (1995) in a 1-Dim box-model, Wyant et al. (1988), and Pujol and Llebot (1999a) in 1-Dim diffusive models, Shutts (1981) in a two-level quasi-geostrophic model, and Paltridge (1978), and Mobbs (1982) in 2-Dim models.

However, the material rate of entropy production only represents one part of the total rate of entropy production (i.e., material plus radiation). With reference to the radiative contribution and based on one of Planck's studies (Planck, 1913), Essex (1984) obtains that an atmosphere in radiative equilibrium would achieve the state with minimum rate of radiative entropy production. Although in a given latitudinal point the atmosphere is not in radiative equilibrium (i.e., both convection and advection are not negligible), this principle has been applied in a 1-Dim box-model (Pujol and Llebot, 1999b), producing reasonable results.

Finally, some authors suggest that the total rate of climatic entropy production (i.e., material plus radiation) is maximum, in agreement with a universal requirement of entropy increase in the universe (Ozawa and Ohmura, 1997). In particular, this principle has been applied in a simple 1-Dim box-model (Pujol and Llebot, 1999b).

In this paper, the climate in a 2-Dim model has been obtained by separately applying the hypothesis of extremal rate of total, material and radiative entropy production. Previous to show the results, however, we must define the expressions of entropy production that have been extremized.

The rate of total entropy production only contains the radiation flux of entropy across the planetary boundaries. Moreover, the radiation flux can be divided into long- and short-wave parts. The main contribution to total entropy production is that due to long-wave radiation because of its low temperature of emission (~ 288 K). By assuming both atmospheric T_a (as calculated by O'Brien and Stephens, 1995) and surface T temperatures as the characteristic ones for the atmosphere and ocean respectively, the normalized (i.e., divided by F) long-wave entropy radiation flux σ_{iLW} reads

$$\sigma_{iLW} = \frac{4}{3} \frac{\eta(C - Dg) - \eta(R - Sg)}{T_a} + \frac{4}{3} \frac{\eta(R - Sg)}{T}, \quad (19)$$

taking into account that $\sigma_{iLW} \approx (4/3)\Delta H/T_c$ (Pujol and Llebot, 1999b), T_c being the characteristic temperature of the region (atmosphere T_a or ocean T), and ΔH the difference of energy fluxes between the upper and the lower levels of the region. Therefore, the first term on the r.h.s. in (19) represents the total entropy production generated in the atmosphere, whereas the last term refers to the contribution produced in the ocean (note that if T_a was equal to T , equation (19) would only contain the entropy radiation flux produced at TOA, as is the case for the short-wave radiation terms).

Total long-wave entropy production is considerably higher than that corresponding to the normalized (i.e., divided by F) incoming short-wave entropy radiation at TOA σ_{iSWi} , being (Li and Chýlek, 1994)

$$\sigma_{iSWi} = -\frac{4}{3} \frac{\varepsilon}{T_s}, \quad (20)$$

where T_s represents the Sun photosphere temperature (~ 5777 K).

The reflected short-wave entropy radiation at TOA σ_{iSWr} is found to depend not linearly on the TOA albedo (Stephens and O'Brien, 1993), being

(normalized by the solar “constant” F)

$$\sigma_{iSWr} = \frac{4}{3} \frac{\varepsilon}{T_s} (\vartheta \psi(\omega^c) + (1 - \vartheta) \psi(\omega^g)), \quad (21)$$

where the ψ function is

$$\psi(\omega^{c,g}) = \omega_{ct,gt} (u \log(2\omega_{ct,gt} \Omega \varepsilon \pi) + v - u), \quad (22)$$

with $u = -0.277$, $v = 0.965$, and Ω the solid angle subtended by the Sun ($\approx 2.17 \times 10^{-5}$).

Thus the rate of total entropy production σ_t (i.e., $\sigma_{iLW} + \sigma_{iSWi} + \sigma_{iSWr}$) in the simple box-model analyzed, is expressed as

$$\begin{aligned} \sigma_t = & \frac{4}{3} \frac{\eta(C - D\vartheta)}{T_a} - \frac{4}{3} \eta(R - S\vartheta) \left(\frac{1}{T_a} - \frac{1}{T} \right) \\ & - \frac{4}{3} \frac{\varepsilon}{T_s} (1 - \vartheta \psi(\omega^c) - (1 - \vartheta) \psi(\omega^g)). \end{aligned} \quad (23)$$

In contrast to σ_t , the material entropy production σ_m related to the climatic system follows a Gibbs equation, leading to

$$\sigma_m = \frac{\zeta_a}{T_a} + \frac{\zeta_o}{T} + q \left(\frac{1}{T_o} - \frac{1}{T} \right). \quad (24)$$

We stress that eq. (24) has been obtained by applying the typical flux-force relationship used in classical non-equilibrium thermodynamics, which is a common assumption in thermodynamic climate models (Nicolis and Nicolis, 1981).

Although (24) takes all the material dissipation processes into account within the box-model used (atmospheric advection, oceanic advection and convection), several authors have applied an extremal principle related to

$$\sigma_p = \frac{\zeta}{T_a}, \quad (25)$$

which only considers the advective dissipation (Paltridge, 1975, 1978; Grassl, 1981; O’Brien and Stephens, 1995).

Finally, the radiative entropy production σ_r can be obtained from (23) and (24), because $\sigma_t = \sigma_m + \sigma_r$. Eqs. (23), (24) and (25) depend on temperature T , cloud-cover ϑ and horizontal heat fluxes ζ , because T_a is a function of T and ϑ (O’Brien and Stephens, 1995). However, from (15) and (16), the above expressions become only a function of ζ . Then, the horizontal heat flux ζ is obtained as that which extremizes σ_t , σ_m , σ_p or σ_r (depending on the assumption considered). Moreover, it is important to notice that temper-

ature and cloud-cover distributions are obtained through specifying the entire horizontal divergence of heat fluxes in a particular box, a more detailed description of the advective transport being unnecessary.

In a 1-Dim model, the extremization procedure can be easily solved by using the method of Lagrange’s multipliers (O’Brien and Stephens, 1995). However, in a 2-Dim model this method is not feasible because the number of Lagrange’s multipliers becomes higher than 1. The only previous reference to a box-model similar to that used here, is in Paltridge (1978), who obtains a simulation for present conditions in a 2-Dim horizontal box-model formed by 400 boxes (20×20) through maximizing σ_p . Paltridge starts with an arbitrary set of the cross-box flows and then, the flow between two adjacent boxes is varied and held at the point of maximum entropy production for those two boxes. Each of the cross-box flows is varied in the same manner. The process is repeated for all the boxes in the model until the global entropy production stops increasing. In order to save computational time, this procedure has been changed. Here, we start with a global picture of the system, where all the parameters are globally-averaged. In this case, from (15) and (16) it is straightforward to obtain both globally-averaged temperature and cloud-cover due to for this particular case the horizontal heat flux vanishes. The following step consists of dividing the system into two equal sections. In each one, the rate of entropy production to be extremized (σ_t , σ_m , σ_p or σ_r) is expressed as a function of the divergence of the horizontal heat flux in that box. Moreover, the total heat flux at both boxes is known from the previous step, so the extremization procedure for both boxes is reduced to finding the extremum in one dimension. (Related to this problem, O’Brien and Stephens (1995) have proved that the solution of the maximization process in a 1-Dim model is unique.) Once the value of the heat flux which extremizes the entropy production has been obtained, both temperature and cloud-cover for those two boxes can be evaluated. The following step is an iteration of the previous step. Thus, once all the variables for one step are known, the extremization procedure can be expanded into a new subdivision. This procedure requires 10 steps in order to achieve a division of the entire globe into 1024 boxes ($= 2^{10}$). The main benefit of such

a process is the short computational time required for the calculus. However, the final result is expected to depend on how we have divided the global system. For example, the results obtained if the zero-dimensional picture of the model is first subdivided in latitude (i.e., providing two hemispheres) and then subdivided in longitude (i.e., providing four divisions of equal surface area, each one with latitude varying from 0° to 90°), differ from those obtained if the first subdivision is in longitude (i.e., providing two divisions each one with latitude ranging from -90° to 90°), and the following subdivision is in latitude (i.e., providing four divisions of equal surface area, each one with latitude varying from 0° to 90°). The reason of this effect is that the multiple non-linear equations applied for solving the model involve parameters that vary both in latitude and in longitude. Therefore, the results differ if the non-linear equations are applied to regions with equal surface area but with different ranges of latitude and/or longitude (due to the average values for the parameters involved in the equations are different). Due to the result for the following subdivision depends on the value obtained in the previous step, the final result (i.e., at 1024 boxes) becomes a function of how we have subdivided the model. However, between all the possible structures (i.e., methods of subdivision), we have chosen that which produces the highest value of σ_t , σ_m or σ_p (when the maximum hypothesis is applied to σ_t , σ_m or σ_p , respectively), or the lowest value of σ_r (when the minimum hypothesis is applied to σ_r).

When the ice-albedo feedback is included in the model, the extremization procedure is similar to that described above. However, before increasing the number of subdivisions, the value of surface albedo is changed in relation to the surface temperature reached by the cell (via eq. (14)) and the process is repeated until the differences between two consecutive steps are lower than $\pm 10^{-4}$ K.

3. Present state

The values of the parameters for current conditions have been chosen as those shown in Subsection 2.2.

3.1. Variable cloud-cover

In this case, both maximum convection and dissipation hypotheses have been used. The maximum dissipation hypothesis has been applied to the rate of total entropy production σ_t , of material entropy production σ_m or of that expression defined by Paltridge σ_p , which represents the advective part of material entropy production. The model does not produce any reasonable result when the rate of radiative entropy production σ_r is minimized. In comparison, a 1-Dim zonally-averaged model is able to obtain results at the minimum in σ_r (Pujol and Llebot, 1999b).

3.1.1. Results. Globally-averaged results obtained by using the ice-albedo feedback are shown in Table 2. Mean planetary values for the three expressions extremized are similar to those obtained by observations (shown in the last column of Table 2), although some differences appear in globally-averaged cloud fraction.

Although globally-averaged values reasonably agree with observations, zonally-averaged results do not fit with observed distributions. For example, the zonally-averaged temperature shown in Fig. 3 behaves less latitudinally homogeneous than real data.

On the other hand, the distribution of cloud-cover (Fig. 4) shows a type of behaviour similar to that obtained by the observations (Chen and Roeckner, 1997). This, a priori, unexpected result due to the simple thermodynamic model used, is

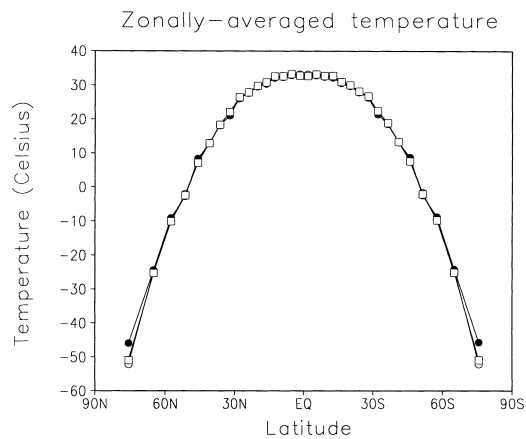


Fig. 3. Zonally-averaged temperature by maximizing σ_p (open circles), σ_m (closed circles) and σ_t (open squares).

Table 2. Globally-averaged values obtained by using different extremal hypotheses; T temperature, ϑ cloud-cover, $LE + H$ latent plus sensible heat fluxes, H_{LT} long-wave radiation fluxes at top of the atmosphere, α_p planetary albedo, σ_p rate of advective entropy production, σ_m rate of material entropy production and σ_t rate of total entropy production; case with variable cloud-cover

Variable	Expression extremized			Observations
	σ_p	σ_m	σ_t	
T (K)	286.7	287.0	286.7	288 ¹
ϑ	0.583	0.615	0.586	0.622 ²
$LE + H$ ($W m^{-2}$)	99.2	99.3	99.2	99.4 ¹
H_{LT} ($W m^{-2}$)	240.2	240.2	240.2	240 ³
α_p	0.300	0.305	0.301	0.300 ³
σ_p ($W m^{-2} K^{-1}$)	0.003	0.004	0.003	0.007 ¹
σ_m ($W m^{-2} K^{-1}$)	0.067	0.069	0.067	0.071 ¹
σ_t ($W m^{-2} K^{-1}$)	1.207	1.207	1.207	1.23 ⁴

¹From Peixoto and Oort (1992).

²From Chen and Roeckner (1997).

³From Hartmann (1994).

⁴From Stephens and O'Brien (1993).

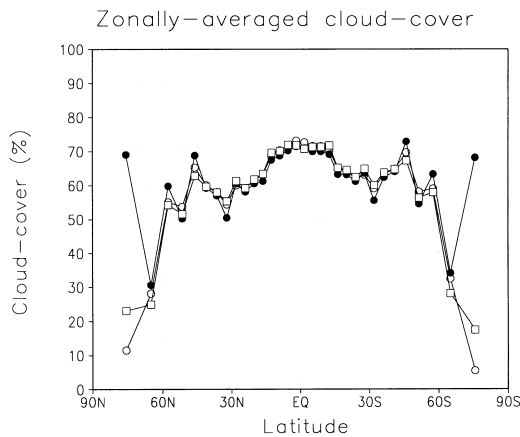


Fig. 4. Zonally-averaged cloud-cover by maximizing σ_p (open circles), σ_m (closed circles) and σ_t (open squares).

a consequence of using a prescribed value of surface albedo, which becomes a fundamental parameter in defining the climate reached by the model (Mobbs, 1982). In contrast to temperature, the zonally-averaged distribution of cloud-cover at high latitudes differs substantially in relation to the expression extremized. Thus, the state of maximum σ_m produces a high value of cloud fraction at both pole-boxes, whereas the maximum in σ_t or in σ_p attains a low value. At low latitudes, the short-wave radiation is clearly a surplus and, in

consequence, the cloud-cover distribution mainly depends on surface albedo for any of the expressions extremized (i.e., a high (low) surface albedo implies a low (high) cloud-cover). However, at high latitudes, there is a deficit of short-wave radiation and, then, the influence of the surface albedo distribution in cloud-cover diminishes in relation to that caused by the application of a specific extremization procedure. Therefore, because σ_t is dominated by the long-wave radiation, the cloud-cover which maximizes σ_t corresponds to a small value. In contrast, because σ_m at high latitudes is dominated by the advective transport, the cloud-cover which maximizes σ_m at these regions reaches great values since the convergence of horizontal heat fluxes and, in consequence, the energy required for convection, increases. This behaviour is directly opposed to that obtained for σ_p since this parameter includes an atmospheric temperature T_a where the cloud-cover plays a key role. It must be pointed out that changes in long- and short-wave parameters used in the model could produce results that were closer to the observed data. However, our interest is not based on calibrating the extremal climate as that observed for current conditions, mainly because, a priori, there is no any reason to conclude that both climates (extreme and real) have to coincide. Therefore, the parameters have been chosen as those used by Paltridge (1978).

Moreover, the distribution of surface temperature practically does not vary in longitude, as can be seen from Fig. 5. Also, the distribution is less latitudinally homogeneous than current data. Cloud fraction distribution at both maximum convection and dissipation is shown in Fig. 6. A

minimum has been found in desert regions where the surface albedo is substantially high. However, at high latitudes where the ice-albedo dominates, the maximum states in σ_p or in σ_t produce a low cloud-fraction, whereas the maximum state in σ_m generates a high value. In all the cases, an

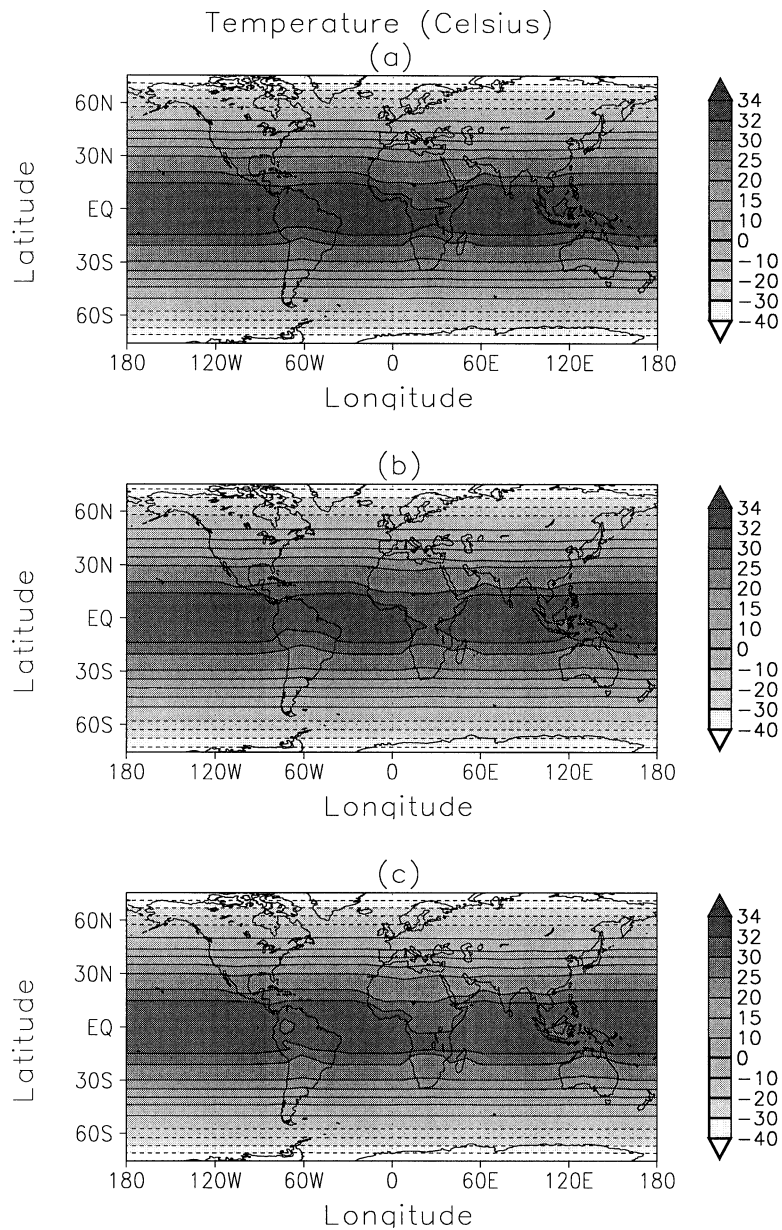


Fig. 5. Distribution of temperatures ($^{\circ}\text{C}$) by (a) maximizing σ_p , (b) maximizing σ_m and (c) maximizing σ_t .

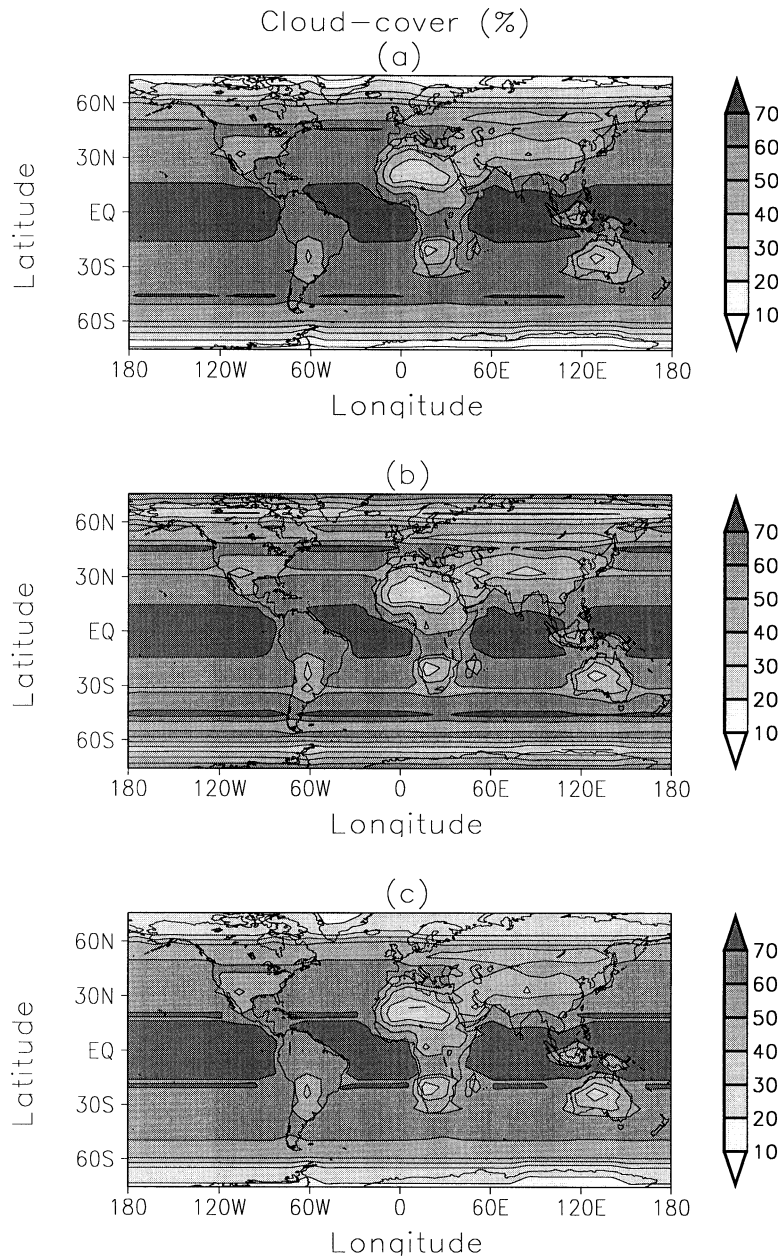


Fig. 6. Distribution of cloud-cover (%) by (a) maximizing σ_p , (b) maximizing σ_m and (c) maximizing σ_t .

equatorial oceanic band with a high cloud fraction has been found, which has been also obtained in a narrow band at mid-latitudes ($\sim 45^\circ$) for the states of maximum σ_p and σ_m . In comparison, the

observed cloud-cover distribution reaches maximum levels in oceanic mid-latitudes, with very low values observed at very high latitudes (Hartmann, 1994).

3.1.2. *Comparison with previous results.* Zonally-averaged results at maximum convection and dissipation obtained by using a 1-Dim version of the model used (10 boxes), are similar for the temperature field (i.e., Fig. 3). However, some discrepancies appear in cloud-cover, especially at high latitudes. Thus, 1-Dim simulations produce a high value of cloud fraction at both pole-boxes (from 53.1° to 90° in the 1-Dim model). In this case, the differences are due to the more detailed discretization in the 2-Dim model, where the ice-covered regions have a characteristic ice-albedo, without being an average value for a broad zone. Moreover, the 2-Dim model cannot simulate a climate at the minimum rate of radiative entropy production as the 1-Dim model does (Pujol and Llebot, 1999b). Thus, the increase in the resolution of the model becomes a constraint in the fulfilment of this hypothesis. Indeed, Essex (1984), based on Planck's results (Planck, 1913), demonstrates that the steady state of a gray atmosphere with matter at rest (i.e., neither advection nor convection) corresponds to a state of minimum radiative entropy production σ_r . Nevertheless, although a detailed picture of the climate must consider both advective and convective fluxes, a global picture of the system could satisfy the constraints required for the success of this hypothesis. In the present analysis, however, besides the extremization of the entropy production, we have applied the convective hypothesis, where the free-variables are those which maximize the convection. Thus, this hypothesis conflicts with the requirements for the acceptance of the minimum principle in σ_r , so the 2-Dim model is not able to produce a feasible climate under such conditions.

3.2. Fixed cloud-cover

The values of the parameters for current conditions are those shown in Subsection 2.2 and used in the previous section. In this case, the extremal dissipation principle (related to σ_t , σ_m , σ_r or σ_p indistinctly) has been applied to the same 2-Dim model but with fixed cloud-cover. Thus, the free-variables in the model are; temperature, latent-plus sensible-heat fluxes and advective fluxes. Due to the cloud-cover has been fixed, the convective hypothesis becomes unnecessary. For comparative purposes, cloud-cover distributions are taken as those obtained in Fig. 6, when the hypothesis of

maximum σ_t , σ_m or σ_p was applied in a model with variable cloud-cover. In contrast to Section 3.1, a simulation at the minimum state in the rate of radiative entropy production σ_r has been obtained. The cloud-cover distribution for this state has been chosen as equal to that obtained in Fig. 6 at the maximum in σ_t or, also, in σ_m , which showed great differences at high latitudes (see cases (b) and (c) in Fig. 6).

3.2.1. *Results.* Globally-averaged results at maximum states in σ_t , σ_m and σ_p , and minimum in σ_r by using the ice-albedo feedback, are shown in Table 3. In comparison with Table 2, the mean planetary temperature varies $\approx 1^\circ\text{C}$ in function of the expression extremized.

Changes in cloud-cover distribution can modify the results. Thus, Table 4 shows the globally-averaged results when the expressions extremized use a cloud-cover distribution related to a different case obtained in Subsection 3.1. For this analysis, the cloud-cover distribution at the maximum state in convection and in σ_p has not been considered because of its similarities to the cloud fraction at the maximum state in convection and in σ_t (Fig. 6). In general, an increase in cloud-cover causes a reduction in temperature, as was expected.

Zonally-averaged distribution of temperature

Table 3. *Globally-averaged values obtained by using different extremal hypotheses; T temperature, ϑ cloud-cover, $LE + H$ latent plus sensible heat fluxes, H_{LT} long-wave radiation fluxes at top of the atmosphere, α_p planetary albedo, σ_p rate of advective entropy production, σ_m rate of material entropy production, σ_t rate of total entropy production and σ_r rate of radiative entropy production; case with fixed cloud-cover and with ice-albedo feedback*

Variable	Expression extremized			
	σ_p	σ_m	σ_t	σ_r
T (K)	287.3	286.8	288.2	285.5
ϑ	0.583	0.615	0.586	0.586
$LE + H$ (W m^{-2})	99.3	99.1	99.8	98.7
H_{LT} (W m^{-2})	240.6	240.1	241.1	239.6
α_p	0.297	0.306	0.293	0.306
σ_p ($\text{W m}^{-2} \text{K}^{-1}$)	0.005	0.004	0.006	0.000
σ_m ($\text{W m}^{-2} \text{K}^{-1}$)	0.069	0.068	0.071	0.064
σ_t ($\text{W m}^{-2} \text{K}^{-1}$)	1.210	1.206	1.215	1.201

for those cases shown in Tables 3–4 are depicted in Figs. 7, 8. In contrast to Fig. 3, notable differences are observed in function of the expression extremized. Thus, the maximum state in total entropy production σ_t tends to be zonally homogeneous, and the minimum state in radiative entropy production σ_r generates a high pole-equator temperature gradient. Although, zonally-averaged temperature distribution at the maximum in σ_t seems to be unrealistic due to the abrupt behaviour depicted in Fig. 7, the results must be seen as a general trend.

Table 4. Similar to Table 3 but with cloud-cover not assumed to be that obtained for the corresponding case with variable cloud-cover

Variable	Expression extremized			
	σ_p	σ_m	σ_t	σ_r
T (K)	286.7	287.1	287.9	285.0
β	0.615	0.586	0.615	0.615
$LE + H$ ($W m^{-2}$)	99.0	99.3	100.2	98.0
H_{LT} ($W m^{-2}$)	240.2	240.4	240.7	239.5
α_p	0.306	0.299	0.302	0.311
σ_p ($W m^{-2} K^{-1}$)	0.004	0.004	0.005	0.000
σ_m ($W m^{-2} K^{-1}$)	0.068	0.068	0.070	0.064
σ_t ($W m^{-2} K^{-1}$)	1.206	1.209	1.211	1.198

For the maximum state in σ_p the distribution of cloud-cover is that obtained through maximizing σ_m for the variable cloud model. For the maximum in σ_m , the cloud-cover is that of the maximum in σ_t ; for the maximum in σ_t and minimum in σ_r , the cloud-cover is that of the maximum in σ_m .

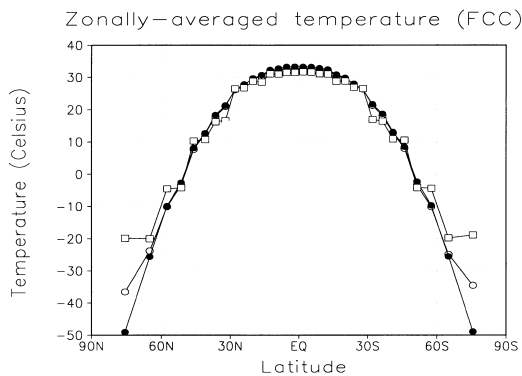


Fig. 7. Zonally-averaged distribution of temperatures with fixed cloud-cover by maximizing σ_p (open circles), σ_m (closed circles) and σ_t (open squares).

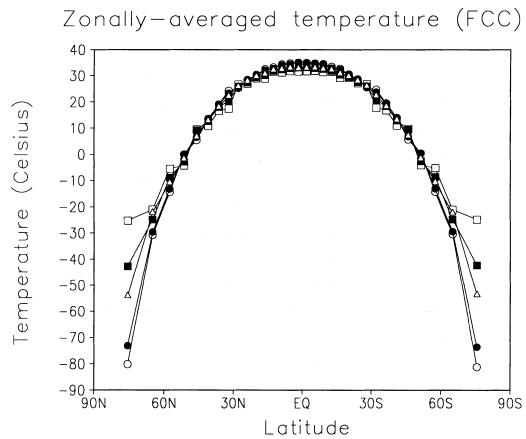


Fig. 8. Zonally-averaged distribution of temperatures by minimizing σ_r with a fixed cloud-cover corresponding to that obtained by maximizing σ_m in the variable cloud model (open circles) or to σ_t (closed circles), by maximizing σ_t with a cloud-cover corresponding to σ_m (open squares), by maximizing σ_m with a cloud-cover corresponding to σ_t (closed squares) and by maximizing σ_p with a cloud-cover corresponding to σ_m (triangles).

When the cloud-cover has been fixed, temperature distributions show more variations in longitude, as can be seen from Fig. 9. However, the simulated temperature distribution is essentially zonal and, therefore, unrealistic. The simplicity of the model used (horizontal flat model with advective heat fluxes obtained through extremal hypotheses that do not depend on the Earth's rate rotation) would be the reason of such a poor representation of the surface temperature distribution. Nevertheless, as Mobbs (1982) points out, the invariance to Earth rotation is an intrinsic problem of the energy balance model used and not of the extremal dissipation principle applied.

The maximum state in σ_t (Fig. 9) contains few regions with temperatures below $-20^\circ C$. Abrupt changes in temperature in a narrow band of latitude follow the type of behaviour commented on in Fig. 7. The maximum state in σ_m produces a latitudinal distribution similar to that obtained by also applying the hypothesis of maximum convection (i.e., by accepting a variable cloud-cover, Fig. 5). The maximum state in σ_p becomes more homogeneous than the preceding one, without reaching values lower than $-40^\circ C$. Finally, the minimum state in σ_r has an important latitud-

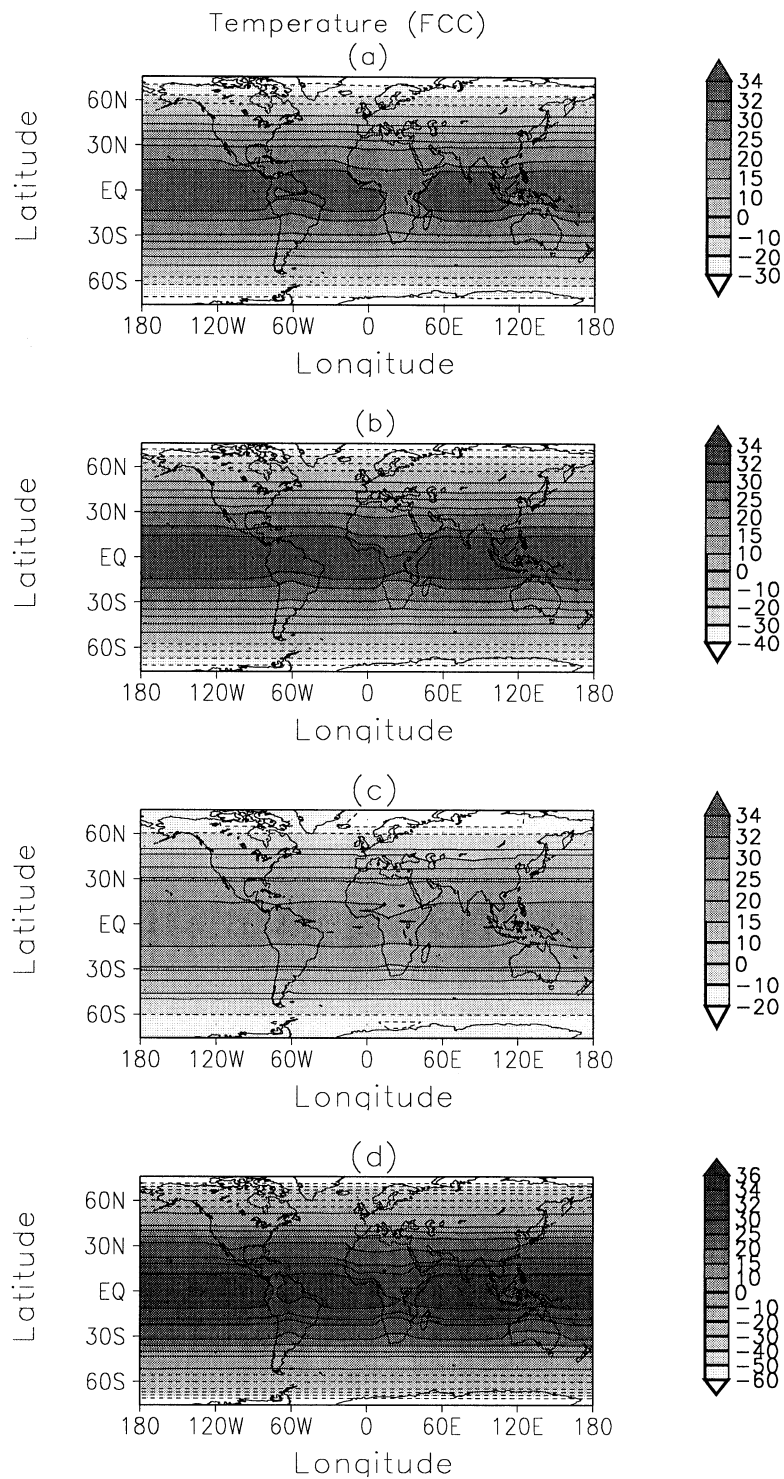


Fig. 9. Distribution of temperatures ($^{\circ}\text{C}$) by (a) maximizing σ_p , (b) maximizing σ_m , (c) maximizing σ_t and (d) minimizing σ_r . Simulations with fixed cloud-cover.

inal temperature gradient, with the pole-boxes below -70°C and equatorial values above 36°C .

3.2.2. *Comparison with previous results.* The equations that govern the 2-Dim model with fixed cloud-cover are similar to those corresponding to EBM diffusive models (i.e., without the maximum convection hypothesis; Hyde et al., 1990). Therefore, the application of several extremal dissipation hypotheses can be compared with those results found by Pujol and Llebot (1999a) in the analysis of a diffusive 1-Dim model, where the maximum state in σ_t becomes isothermal and the maximum in σ_m more homogeneous than current values. In consequence, the structure of the model can cause changes in the results although the basic characteristics are maintained. For example, the maximum in σ_t with fixed cloud-cover tends to be more homogeneous than the maximum state in σ_m (Fig. 9).

4. Climatic sensitivity

The climatic sensitivity generated by the 2-Dim model has been obtained by varying the parameters described in Section 2. Moreover, calculations have been carried out with and without prescribed cloud-cover, as well as with and without the ice-albedo feedback.

4.1. Variable cloud-cover

Variations in surface temperature T , cloud-cover ϑ , long-wave radiation flux at TOA H_{LT} , and planetary albedo α_p ($\alpha_p = \omega_{gt}(1 - \vartheta) + \omega_{ct}\vartheta$) due to changes in any of the parameters used in the simple 2-Dim model are shown in Table 5 with and without ice-albedo feedback at the maximum rate of material entropy production σ_m . The variations have been normalized by the change in the parameter itself, so the results can be compared directly. Temperature and cloud-cover are highly dependent on the long-wave parameters m_c and m_g as well as on the values assumed for the short-wave parameter ω_c . Moreover, an increase in cloud albedo ω_c causes an increase in temperature. This type of behaviour is a result of the convective hypothesis. Thus, it is reasonable to suppose that the extremal state depends on both global cloud-

Table 5. Global sensitivity to changes in the parameters of the model; case with and without ice-albedo feedback and maximizing σ_m (with variable cloud-cover)

p	Without the ice-albedo feedback				With the ice-albedo feedback			
	$\Delta T/\Delta \ln p$	$\Delta \vartheta/\Delta \ln p$	$\Delta H_{LT}/\Delta \ln p$	$\Delta \alpha_p/\Delta \ln p$	$\Delta T/\Delta \ln p$	$\Delta \vartheta/\Delta \ln p$	$\Delta H_{LT}/\Delta \ln p$	$\Delta \alpha_p/\Delta \ln p$
m_g (+10%)	-34.8	135	-90.4	26.6	-34.4	127	-87.9	24.5
m_h (+10%)	7.1	-43	74.6	-17.5	8.2	-71	81.2	-25.6
m_c (-1%)	-44.2	-188	18.2	-16.7	-50.7	-209	-2.7	5.7
ω_g (+5%)	-11.6	27	-36.4	10.0	-9.1	75	-33.5	9.8
ω_c (+5%)	24.2	-153	86.8	-21.0	27.4	-151	93.8	-28.6
ω_g (+10%)	-0.3	-6	-0.3	-0.4	0.9	22	1.2	-0.6
ω_c (+10%)	1.7	18	4.0	-0.6	2.2	19	5.6	-2.2
α_a (+10%)	0.3	-7	0.9	-1.1	1.2	23	2.3	-1.0
α_c (+10%)	10.6	-29	36.0	-8.9	11.3	-27	38.3	-11.4
F -16 W m ⁻²	71.6	0	239.1	0	64.4	-154	227.7	6.1

cover and clear-sky albedos. Furthermore, the new extremal state reached by the system when a given parameter slightly varies, can be expected to be close to the initial one. In consequence, when a parameter is modified, the variation in cloud-cover is that which tends to reduce the variation in the global albedo caused by the change in the parameter. Therefore, an increase in ω_c implies a substantial decrease in \mathcal{G} , which becomes enough to cause an increase in temperature.

Results at the maximum rate of advective material entropy production σ_p are similar to those shown in Table 5, whilst those at the maximum rate of total entropy production σ_t display some differences. In this case, the sensitivity of temperature is greater than in Table 5, whereas changes in cloud-cover are smaller.

4.2. Fixed cloud-cover

Changes in surface temperature T , long-wave radiation at TOA H_{LT} , and planetary albedo α_p , with and without ice-albedo feedback when the cloud-cover has been fixed and the parameters have been modified, are shown in Table 6, where the climatic variations correspond to maximum states in σ_m . When the ice-albedo feedback has not been taken into account, changes in long-wave parameters do not cause variations in H_{LT} as well as in α_p , because the short-wave parameters do not change (cloud-cover fixed). The introduction of the ice-albedo feedback causes an increase in the variations of temperature because of the sensitivity of the model to changes in surface albedo. However, for changes in surface emissivity

m_g , the variations become smaller in comparison with the climatic sensitivity at the maximum convection and dissipation. Thus, climatic variations at maximum dissipation when the cloud-cover is fixed, are shorter than those observed when cloud fraction is obtained through applying the convective hypothesis in agreement with a similar study carried out by Manabe and Broccoli (1985). Moreover, because the cloud-cover has not been obtained through the convective hypothesis, an increase in cloudy as well as in clear-sky albedo implies a reduction in temperature.

5. Conclusions

It is desirable that the thermodynamic state of a system corresponds to the extreme value of some function. Based on this idea, the possible extremal behaviour for the climatic system has been analyzed by using a 2-Dim horizontal box-model subdivided into oceanic and atmospheric parts. The extremal hypothesis has been related to the rate of entropy production, which appears to be a suitable variable in comparison with classical thermodynamic systems (Prigogine, 1947). However, the existence of both radiative and material fields in the climatic system complicates the theoretical analysis and makes difficult a fully demonstration of the extremal assumption. Therefore, if the extremal behaviour of the climatic system cannot be analytically verified, the extremal hypothesis must be applied to several climatic models in order to investigate its validity. Moreover, several points must be taken into

Table 6. Global sensitivity to changes in the parameters of the model; case with and without ice-albedo feedback and maximizing σ_m (with fixed cloud-cover)

p	Without the ice-albedo feedback			With the ice-albedo feedback		
	$\Delta T/\Delta \ln p$	$\Delta H_{LT}/\Delta \ln p$	$\Delta \alpha_p/\Delta \ln p$	$\Delta T/\Delta \ln p$	$\Delta H_{LT}/\Delta \ln p$	$\Delta \alpha_p/\Delta \ln p$
m_g (+10%)	-13.4	0	0	-14.1	-1.4	0.8
m_a (+10%)	-14.0	0	0	-14.6	-1.5	0.9
m_c (-1%)	-44.2	0	0	-45.6	-3.0	1.7
ω_g (+5%)	-2.9	-9.3	2.8	-3.2	-9.9	3.2
ω_c (+5%)	-19.3	-64.3	18.4	-20.1	-66.3	19.8
ω_g (+10%)	0.4	1.1	-0.4	0.3	1.0	-0.4
ω_c (+10%)	1.3	4.0	-1.4	1.2	3.8	-1.3
α_a (+10%)	1.1	3.3	-1.2	1.0	3.2	-1.1
F -16 W m ⁻²	71.9	238.8	0	74.6	245.9	-3.2

account in order to elucidate the success of an extremal principle, e.g.: (1) the climate obtained by applying the extremal hypothesis must produce similar results to the observations and to those simulated by complex climatic models (e.g., GCM), which are assumed to properly describe the climate due to consider a great quantity of mechanisms that govern the system; (2) the results of applying an extremal principle must be invariant on the dimension and structure of the climatic model used; of course, changes in the results are expected if the model is an EBM (like that used here) or explicitly includes the dynamics of the system; however, the basic features obtained through applying the extremal hypothesis must remain; (3) although no demonstrations can be provided for the application of an extremal principle, it should be based on reasonable assumptions.

Here, climatic simulations at the maximum rate of total entropy production σ_t (i.e., material plus radiative contributions), of material entropy production σ_m and of the advective part of material entropy production σ_p , as well as at the minimum rate of radiative entropy production σ_r , have been carried out. The hypothesis of maximum convection has been also analyzed, which asserts that the system tends to reach a state that maximizes the convective fluxes.

The 2-Dim model used is a version of Paltridge's 1-Dim box-model extensively applied in these types of studies (Paltridge, 1975; 1978; 1981; Grassl, 1981; O'Brien and Stephens, 1995; Pujol and Llebot, 1999b). Although Paltridge (1978) already analyzes a 2-Dim version, the model developed consists of more boxes ($1024 = 32 \times 32$) and uses a different method of solution. In this simple EBM, four free-variables are defined in each box; temperature, cloud-cover, advective fluxes and convective fluxes, which are solved by applying both maximum convection and entropy production hypotheses (related to σ_t , σ_m or σ_p). When the cloud-cover has been fixed, the three free-variables are obtained by applying the extremal condition of entropy production (related to σ_t , σ_m , σ_r or σ_p). Both cases are simulated with and without the ice-albedo feedback. Current conditions for the parameters are chosen similar to those considered by Paltridge (1978), where the surface albedo is the only parameter that varies in longitude as well as in latitude.

The temperature distribution at the maximum state in convection and dissipation becomes similar for the different expressions analyzed (maximum in σ_t , σ_m or σ_p), being less latitudinally homogeneous than real data. Some differences appear in the distribution of cloud-cover. The maximum states in σ_t and in σ_p generate a reduced amount of cloud at high latitudes in contrast to the values obtained at the maximum in σ_m . In comparison with previous 1-Dim results, the increase in the dimension of the model does not imply relevant changes in the basic structure of the solutions (Paltridge, 1978; O'Brien and Stephens, 1995; Pujol and Llebot, 1999b). The simulations carried out keeping constant the distribution of cloud-cover, and being equal to that obtained for the cases at maximum convection, are clearly dependent on the extremal hypothesis of entropy production. Thus, the maximum state in σ_t reduces the pole-equator temperature gradient. The maximum in σ_m (or in σ_p) is similar to that obtained when both convective and dissipative hypotheses have been applied. Finally, the minimum state in σ_r has an extreme temperature gradient in latitude. Moreover, simulations with fixed cloud-cover produce more variations in longitude than those obtained when the cloud-cover was deduced from the convective hypothesis. In comparison with current data, however, the results are unrealistic due to the simple formulation of the model.

Thus, the convective hypothesis appears to be fundamental for generating the cloud-cover reached by the system, which modulates the temperature distribution and, in consequence, being slightly dependent on the principle of maximum dissipation applied.

The climate model with fixed cloud-cover can be compared with results obtained by using simple diffusive EBMs, where extremal dissipation principles have been introduced (Pujol and Llebot, 1999a). Thus, the structure of the model can modify the results obtained, although the main characteristics of the results remain invariable (i.e., state latitudinally more and less homogeneous by maximizing σ_t and σ_m respectively).

A sensitivity analysis has been also carried out for both fixed and variable cloud models. Changes in globally-averaged temperature, cloud-cover, long-wave radiation at TOA and planetary albedo

in function of changes in the parameters used in the model have been shown.

To conclude, the present paper has been focused on (1) the dependence of extremal principles on the structure and dimension of the model, (2) the role of the convective hypothesis in defining the states reached by the system, and (3) the effect of the ice-albedo feedback in the extremal states. The results appear to infer a feasible application of the maximum rate of total entropy production σ_t plus maximum convection. Moreover, reasonable results are also obtained by applying the hypothesis of maximum rate of material entropy production σ_m , although the cloud-cover at high latitudes does not correspond with the observations. Nevertheless, the similarity of the simulated climate for both fixed and variable cloud-cover states, supports the possible validity of the maximum dissipation hypothesis in σ_m . Furthermore, the maximization of this expression has produced reasonable results in defining the vertical temperature distribution in a simple climate model (Ozawa and Ohmura, 1997). However, the application of this principle to simple 1-Dim diffusive models does not produce satisfactory results, maybe because such models neglect the contribution of convective fluxes, whose contribu-

tion to σ_m is about $10\times$ greater than that due to advective fluxes (see Peixoto and Oort, 1992). Nevertheless, we comment on the reasonable results obtained by Wyant et al. (1988) who applied the maximum principle in σ_m to several time-dependent 1-Dim diffusive models (Wyant et al.'s procedure is slightly different than that used here, since they assume a diffusive approach for the heat fluxes and apply the extremal principle in order to obtain the planetary "diffusivity").

However, since no theoretical demonstrations for any of the extremal hypotheses have been obtained, a more exhaustive analysis is required in order to support their possible applications to the climate. In Part II several simulations for pre-industrial conditions and possible future scenarios have been carried out, including both aerosol and greenhouse gas effects, from where the application of the maximum dissipation principle in σ_m appears to be questionable.

6. Acknowledgements

This work has been partially supported by the Ministerio de Educación y Cultura of the Spanish Government under contract PB96-0451.

REFERENCES

- Chen, C.-T. and Roeckner, E. 1997. Cloud simulations with the Max Planck Institute for Meteorology general circulation model ECHAM4 and comparison with observations. *J. Geophys. Res.* **102**, 9335–9350.
- Essex, C. 1984. Minimum entropy production in steady state and radiative transfer. *Astrophys. J.* **285**, 279–293.
- Ghil, M. and Le Treut, H. 1981. A climate model with cryodynamics and geodynamics. *J. Geophys. Res.* **86**, 5262–5270.
- Grassl, H. 1981. The climate at maximum entropy production by meridional atmospheric and oceanic heat fluxes. *Q. J. R. Meteorol. Soc.* **107**, 153–166.
- Hartmann, D. L. 1994. *Global physical climatology*, vol. 56. International Geophysics Series, Academic Press, New York.
- Hyde, W. T., Kim, K.-Y., Crowley, T. J. and North, G. R. 1990. On the relation between polar continentality and climate: studies with a nonlinear seasonal energy balance model. *J. Geophys. Res.* **95**, 18653–18668.
- Källén, E., Crafoord, C. and Ghil, M. 1979. Free oscillations in a climate model with ice-sheet dynamics. *J. Atmos. Sci.* **36**, 2292–2303.
- Li, J. and Chylek, P. 1994. Entropy in climate models. Part II: Horizontal structure of atmospheric entropy production. *J. Atmos. Sci.* **51**, 1702–1708.
- Lian, M. S. and Cess, R. D. 1977. Energy balance models: a reappraisal of ice-albedo feedback. *J. Atmos. Sci.* **34**, 1058–1062.
- Manabe, S. and Broccoli, A. J. 1985. A comparison of climate model sensitivity with data from the last glacial maximum. *J. Atmos. Sci.* **42**, 2643–2651.
- Mobbs, S. D. 1982. Extremal principles for global climate models. *Q. J. R. Meteorol. Soc.* **108**, 535–550.
- Nicolis, G. and Nicolis, C. 1981. On the entropy balance of the earth-atmosphere system. *Q. J. R. Meteorol. Soc.* **106**, 691–706.
- North, G. R., 1975. Analytical solution to a simple climate model with diffusive heat transfer. *J. Atmos. Sci.* **32**, 1301–1307.
- O'Brien, D. M. and Stephens, G. L. 1995. Entropy and climate. II: Simple models. *Q. J. R. Meteorol. Soc.* **121**, 1773–1796.
- Ozawa, H. and Ohmura A. 1997. Thermodynamics of a global-mean state of the atmosphere — a state of maximum entropy increase. *J. Climate* **10**, 441–445.
- Paltridge, G. W. 1975. Global dynamics and climate — a system of minimum entropy exchange. *Q. J. R. Meteorol. Soc.* **101**, 475–484.
- Paltridge, G. W. 1978. The steady-state format of global climate. *Q. J. R. Meteorol. Soc.* **104**, 927–945.

- Paltridge, G. W. 1979. Climate and thermodynamic systems of maximum dissipation. *Nature* **279**, 630–631.
- Paltridge, G. W. 1981. Thermodynamic dissipation and the global climate system. *Q. J. R. Meteorol. Soc.* **107**, 531–547.
- Peixoto J. P. and Oort A. H. 1992. *Physics of climate*. AIP, New York.
- Planck, M. 1913. *Heat radiation* (trans.), 2nd edition, republished 1959. Dover, New York.
- Prigogine I. 1947. *Etude thermodynamique des phénomènes irréversibles*. Desoer, Liège.
- Pujol, T. and Llebot, J. E. 1999a. Second differential of the entropy as a criteria for the stability in low-dimensional climate models. *Q. J. R. Meteorol. Soc.* **125**, 91–106.
- Pujol, T. and Llebot, J. E. 1999b. Extremal principle of entropy production in the climate system. *Q. J. R. Meteorol. Soc.* **125**, 79–90.
- Roesch, A., Gilgen, H., Wild, M. and Ohmura, A. 1999. Assessment of GCM simulated snow albedo using direct observations. *Clim. Dyn.*, **15**, 405–418.
- Shutts, G. J. 1981. Maximum entropy production states in quasi-geostrophic dynamical models. *Q. J. R. Meteorol. Soc.* **107**, 503–520.
- Stephens, G. L. and O'Brien, D. M. 1993. Entropy and climate. I: ERBE observations of the entropy production of the earth. *Q. J. R. Meteorol. Soc.* **119**, 121–152.
- Wyant, P. H., Mongroo, A. and Hameed, S. 1988. Determination of the heat-transport coefficient in Energy-Balance Climate Models by extremization of entropy production. *J. Atmos. Sci.* **45**, 189–193.